

EVIDENCE OF NARROW RANGE HIGH SPIN POPULATION IN INCOMPLETE FUSION*

ARSHIYA SOOD^a, PAWAN KUMAR^a, R.N. SAHOO^a
PUSHPENDRA P. SINGH^a, ABHISHEK YADAV^b, VIJAY R. SHARMA^c
MANOJ K. SHARMA^d, R. KUMAR^e, R.P. SINGH^e, S. MURALITHAR^e
B.P. SINGH^f, R.K. BHOWMIK^e

^aDepartment of Physics, Indian Institute of Technology Ropar
Rupnagar-140001, Punjab, India

^bDepartment of Physics, Jamia Milia Islamia, New Delhi-110067, India

^cININ, Apartado Postal 18-1027, CP 11801 Ciudad de Mexico, Mexico

^dDepartment of Physics, S.V. College, Aligarh-202 001, UP, India

^eNP-Group Inter-University Accelerator Center, New Delhi-110 067, India

^fDepartment of Physics, A.M. University, Aligarh-202 002, UP, India

(Received January 7, 2020)

Particle (p, α) - γ -coincidence experiment has been performed to probe incomplete fusion dynamics in the $^{12}\text{C}+^{169}\text{Tm}$ system at 5–7.5 MeV/A. Spin distributions of different reaction products populated via xn and $\alpha/2\alpha xn$ channels have been measured to acquire information about the involved reaction mechanism on the basis of their experimentally observed de-excitation patterns. The spin distributions of direct- α (incomplete fusion) and fusion–evaporation (complete fusion) channels are found to be distinct from each other, substantiating their origin in entirely different reaction dynamics. It has been found that CF products span a broad spin range, while ICF products are confined to a narrow spin range localized in the higher spin states. Findings of the present work comprehensively demonstrate that incomplete fusion reactions can be used as a sensitive tool to populate high-spin states in final reaction products, which are not otherwise accessible.

DOI:10.5506/APhysPolB.51.775

1. Introduction

Incomplete fusion (ICF) is a class of heavy-ion reactions, in which only a fraction of incident projectile coalesces with the target nucleus, while the remaining part escapes at forward angles with almost projectile velocity [1].

* Presented at the XXXVI Mazurian Lakes Conference on Physics, Piaski, Poland, September 1–7, 2019.

ICF reactions involve transfer of one, two or a few nucleons from a lighter projectile to a target and are, generally, characterized by narrow kinetic energy spectra of the projectile-like fragments, showing maxima around the grazing angle and progressively becoming forward peaked with increasing mass transfer. At energies near and above the Coulomb barrier, the complete fusion (CF) — amalgamation of entire projectile with the target nucleus — is a dominant reaction process. The onset of ICF reactions is mostly associated with projectile energies ≥ 10 MeV/ A , where in order to provide sustainable angular momentum for fusion to occur, the projectile breaks up into its constituents, thereby releasing excess driving input angular momentum. However, recent experimental investigations have suggested the onset of ICF at slightly above barrier energies ≈ 4 –7 MeV/ A , where CF is expected to be the sole contributor [2, 3].

Various theoretical models have been put forward to explain these reactions, *viz.* Break-up Fusion (BUF) [4], SUMRULE [5], Promptly Emitted Particles (PEP) [6], Fermijet [7], Overlap [8] and Multistep Direct Reaction [9]. Although these theoretical approaches have passably interpreted the experimental results obtained at energies ≥ 10 MeV/ A , yet there is a dearth of comprehensive understanding of the underlying ICF dynamics particularly at low bombarding energies, *i.e.* $E_{\text{lab}} \approx 4$ –7 MeV/ A .

Some of the outstanding issues related to ICF at these energies are: the localization of input angular momentum window and the possibility of populating high-spin states at low incident energies using ICF reactions. The phenomenon of ICF has been extensively studied for different projectile–target combinations, energy ranges and entrance channel parameters by measurement of excitation functions, recoil range distributions, velocity distribution of evaporation residues, and angular distribution of projectile-like fragments. However, there is a paucity of studies that can furnish direct evidence for the angular momentum associated with various exit channels at energies ≈ 4 –7 MeV/ A . Therefore, for many years now, ICF has attracted resurgent interest and has been an active area of research, in general, and at low energies, in particular, to understand its underlying dynamics and a role in producing heavy and superheavy neutron-rich isotopes [10–12].

To probe the onset of ICF at slightly above barrier energies and possibility of populating high-spin states in residual nucleus, a particle (p, α)– γ -coincidence experiment has been performed to measure the spin distributions of various reaction products populated in $^{12}\text{C}+^{169}\text{Tm}$ in the energy range ≈ 5 –7.5 MeV/ A at 7 different energies.

2. Experimental procedure, results and discussion

The experiments were carried out at the Inter-University Accelerator Center (IUAC), New Delhi (India). $^{12}\text{C}^{5+}$ beams ($E_{\text{lab}} \approx 60$ –90 MeV) from

the 15UD Pelletron Accelerator bombarded an isotopically pure, self-supporting ^{169}Tm target of thickness $\approx 1.8 \text{ mg/cm}^2$. The spin distributions of reaction products populated via $xn, \alpha/2\alpha xn$ channels in complete and incomplete fusion of ^{12}C with ^{169}Tm at $E_{\text{lab}} \approx 5\text{--}7.5 \text{ MeV/A}$ were measured employing the particle $(p, \alpha)\text{--}\gamma$ -coincidence technique. In order to register the coincidences, charged particles were detected in a compact array of scintillators placed inside the Gamma Detector Array (GDA). The GDA is a multi-detector system consisting of 12 Compton-suppressed, high-resolution n -type HPGe detectors. Besides, the Charged Particle Detector Array (CPDA) comprises 14 phoswich detectors. The HPGe detectors were set at angles 45° , 99° and 153° with respect to the beam direction and there were 4 detectors at each angle, while 14 CPDs were categorized into three angular regions embodying four ‘forward’ (F), six ‘sideways’ (S) and four ‘backward’ (B) detectors subtending the angles of $\approx 10^\circ\text{--}60^\circ$, $60^\circ\text{--}120^\circ$ and $120^\circ\text{--}170^\circ$, respectively. The particle $(p, \alpha)\text{--}\gamma$ -coincidences were established by employing different gating conditions corresponding to the aforementioned three angular regions.

The identification of reaction products emanating from CF and/or ICF was done explicitly based on their characteristic prompt gamma rays from the singles and/or gated spectra. The pure CF xn evaporation channels were identified from singles spectra, whereas backward- α -gated and forward- α -gated spectra were analyzed to identify $\alpha/2\alpha xn$ evaporation channels produced via CF and/or ICF. The details of the experiment and data analysis are delineated in Refs. [13, 14].

It is important to mention here that two groups of alpha particles *viz.* fusion-evaporation ‘slow’ alphas and ‘fast’ direct alphas emerging from the CF and ICF process, respectively, are expected to be detected by the F CPDs. Since for the studies of our interest we required only fast alphas to be detected in the forward cone, therefore, it was essential to stop the slow alphas by putting absorbers of sufficient thickness in front of the F CPDs. The energy profiles of the slow alphas for $E_{\text{lab}} \approx 60\text{--}90 \text{ MeV}$ at forward angles were simulated using the statistical model code PACE4 [15]. For instance, the energy profile of slow alphas at $E_{\text{lab}} \approx 90 \text{ MeV}$ and 60 MeV is shown in Fig. 1 (a) and (b), respectively. As can be seen from Fig. 1 (a) and (b), the most probable energy ($E_{\text{CF-}\alpha}$) of slow alphas is found to be $\approx 20 \text{ MeV}$ and 17 MeV , respectively. The energy of fast alphas ($E_{\text{ICF-}\alpha}$) was calculated using the relation $E_{\text{ICF-}\alpha} = E_{\text{P}} \times \frac{M_{\alpha}}{M_{\text{P}}}$, where E_{P} is the projectile energy, M_{α} , M_{P} are the masses of alpha and projectile, respectively. For the ^{12}C beam at 90 MeV and 60 MeV , the calculated value of $E_{\text{ICF-}\alpha}$ is $\approx 30 \text{ MeV}$ and 20 MeV . As such, to detect only fast alphas, Al absorber foils of appropriate thickness were kept in front of all F CPDs to stop slow alphas. Additionally, to remove any contribution of slow CF- α s (indicated by the

extended tail of simulated α spectra towards higher energy side, particularly at lower incident energies, as shown in Fig. 1 (b)) in the forward cone, backward- α -gated spectra were subtracted from the forward- α -gated spectra. The direct- $\alpha xn/2\alpha xn$ channels produced via ICF were then identified from the corrected forward- α -gated spectra.

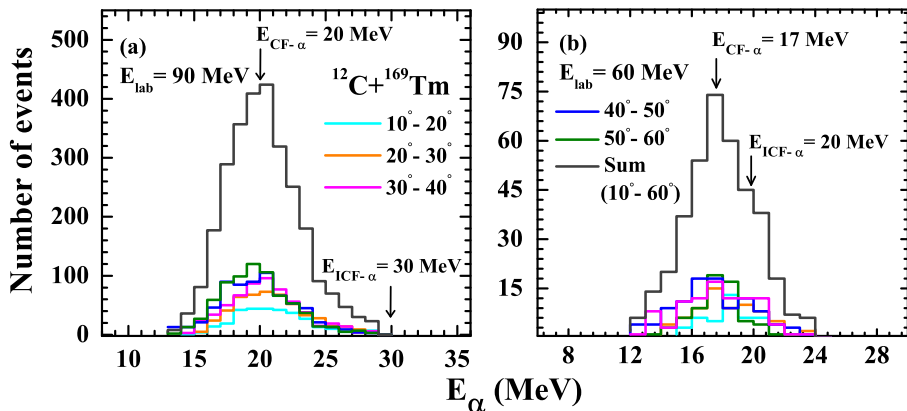


Fig. 1. Energy profiles of fusion–evaporation alphas simulated using the statistical model code PACE4 for the forward (10° – 60°) angular region at $E_{\text{lab}} \approx$ (a) 90 MeV and (b) 60 MeV in the $^{12}\text{C} + ^{169}\text{Tm}$ system.

To understand the decay patterns of CF and ICF reactions and to estimate the input angular momentum associated with a particular reaction channel, spin distributions of different reaction products have been obtained by plotting the relative production yields as a function of experimentally observed spin (J_{obs}) corresponding to the prompt γ transitions. Relative production yields of different reactions channels have been normalized with their respective highest yield values ($Y_{\text{obs}}^{\text{max}}$) corresponding to the lowest observed spin ($J_{\text{obs}}^{\text{min}}$) for better comparison. The experimentally measured spin distributions have been obtained for the xn (^{176}Re), αxn (^{174}Ta) and $2\alpha xn$ (^{171}Lu) channels populated via CF and/or ICF reactions at $E_{\text{lab}} \approx 60$ – 90 MeV. For instance, the spin distributions of the αxn channel identified from backward- and forward-gated spectra are shown in Fig. 2 (a) and (b), respectively.

To determine the value of mean driving input angular momenta for different reaction channels and to have a better analytical representation of data, the lines and curves are drawn through the data points as the least square fits to the function described in Refs. [13, 14].

As apparent from this figure, there is a conspicuous difference between the decay patterns of αxn channels obtained from backward- and forward-gated spectra, manifesting their origin from entirely different reaction mech-

anism. The yields of successively lower transitions in Fig. 2 (a) show an exponential rise towards the band head, indicating strong feeding of lower spin states, which corroborates the general trend of de-excitation of complete fusion reaction products, whereas in Fig. 2 (b), the yields appear to increase down to certain value of observed spin ($J_{\text{obs}}^{\text{min}}$), after which they are constant towards the band head. This indicates the absence of feeding to lower members of the yrast band and/or hindered population of the low-spin states, connoting the population of the α channel via ICF. A similar trend has been observed for all other xn - and α -emitting channels identified from singles, backward- and forward- α -gated spectra [14].

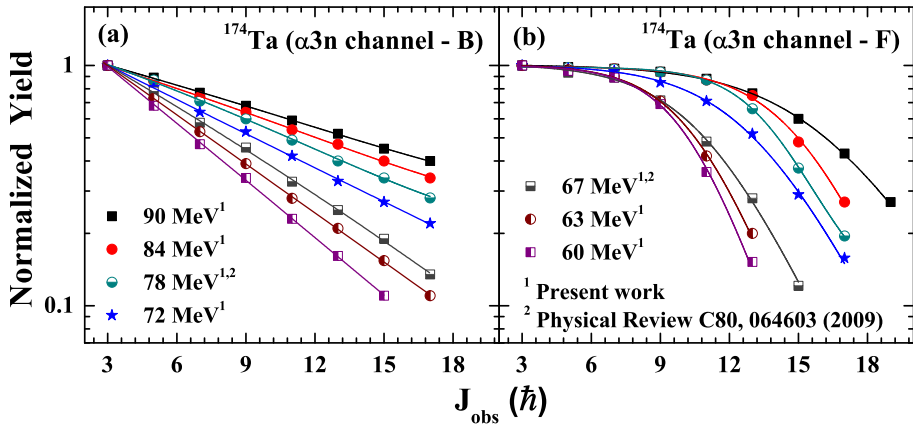


Fig. 2. Experimentally measured spin distributions for ^{174}Ta ($\alpha 3n$ channel) populated in the $^{12}\text{C} + ^{169}\text{Tm}$ reaction at $E_{\text{lab}} \approx 60\text{--}90$ MeV. ‘F’ and ‘B’ represent the reaction products identified from forward- and backward- α -gated gamma-ray spectra, respectively. The curves through data points are least square fits to the function explained in the text.

In order to determine the possibility of selective population of high-spin states in residual reaction products, the mean values of input angular momenta $\langle \ell \rangle$ obtained for the CF- $xn/\alpha xn$ and ICF- $\alpha xn/2\alpha xn$ channels are plotted as a function of projectile energy in Fig. 3. The value of $\langle \ell \rangle$ is found to range from 7–13 \hbar for the CF- xn and $-\alpha xn$ channels, whereas for the ICF- αxn and $-2\alpha xn$ channels, it approaches 10–16 \hbar and 11–18 \hbar , respectively, at $E_{\text{lab}} \approx 60\text{--}90$ MeV. As can be seen from this figure, for the αxn channel identified from the backward- α -gated spectra, the value of $\langle \ell \rangle$ is notably lower than for the direct- αxn channels identified from forward- α -gated spectra. Further, it has been observed that for the ICF- αxn and $-2\alpha xn$ channels, the multiplicity of fast α s increases with the input angular momentum imparted into the system. At a given energy, the $2\alpha xn$ channel is populated

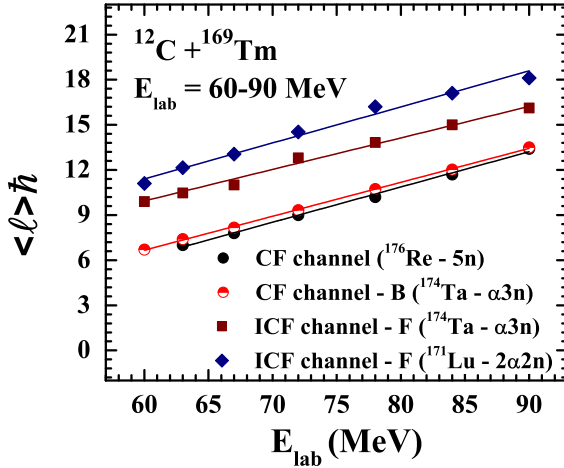


Fig. 3. Mean input angular momenta as a function of projectile energy in the $^{12}\text{C} + ^{169}\text{Tm}$ system. The lines are the linear fits through data points.

at a higher angular momentum than αxn indicating the variation of ℓ bins with impact parameter in ICF reactions. Besides, the value of ℓ associated with the production of the same residue via CF at a higher projectile energy can be achieved via ICF even at a lower projectile energy. For instance, the value of ℓ for ^{174}Ta ($\alpha 3n$ -channel) populated via CF at $E_{\text{lab}} \approx 7.5$ MeV/A is $\approx 13.5 \hbar$, which is reached via ICF ($\approx 14 \hbar$) at a lower projectile energy $E_{\text{lab}} \approx 6.5$ MeV/A. Moreover, ℓ values involved in the production of the ICF- $2\alpha xn$ and $-\alpha xn$ reaction channels are ≈ 35 – 74% and ≈ 20 – 50% higher as compared to the CF- $xn/\alpha xn$ channels, respectively, in the studied energy range. This clearly suggests that at a given projectile energy, higher ℓ values are involved in the production of ICF residues, essentially due to non-central interactions, where a significant amount of orbital angular momentum between projectile and target results in the population of high-spin states in these residues. Thus, the present study strongly supports the possibility of ICF as an advantageous tool to access high-spin states in the residual nucleus even at low projectile energies, which are not possible otherwise.

3. Summary and conclusions

In the present work, spin distributions of reaction products populated via $xn, \alpha/2\alpha xn$ channels in CF and ICF in the $^{12}\text{C} + ^{169}\text{Tm}$ system at $E_{\text{lab}} \approx 5$ – 7.5 MeV/A have been measured. The spin distributions of CF and ICF products are found to be strikingly different, corroborating the involvement of entirely different reaction dynamics in their production. For CF channels,

the yield of successively lower transitions shows an exponential rise towards the band head, indicating strong feeding and/or continuous population of low-spin states, whereas for ICF channels, the yield is constant down to a certain value of J_{obs} , after which it does not change towards the band head, indicating the absence of feeding to the lower members of yrast band and/or that the population of low-spin states is hindered. The analysis of ℓ values involved in the CF and ICF reactions suggests that ICF can populate high-spin states at low projectile energies, which are not otherwise possible to achieve.

Authors thank the Director of IUAC New Delhi, India for providing all the necessary experimental facilities. P.P.S. acknowledges a startup grant from the Indian Institute of Technology Ropar and the Science and Engineering Research Board (SERB), India for Young Scientist Research Grant No. YSS/2014/000250.

REFERENCES

- [1] H.C. Britt, A.R. Quinton, *Phys. Rev.* **124**, 877 (1961).
- [2] C. Gerschel, *Nucl. Phys. A* **387**, 297 (1982).
- [3] P.P. Singh *et al.*, *Phys. Rev. C* **77**, 014607 (2008) and references therein.
- [4] T. Udagawa, T. Tamura *et al.*, *Phys. Rev. Lett.* **45**, 1311 (1980).
- [5] J. Wilczyński *et al.*, *Phys. Rev. Lett.* **45**, 606 (1980).
- [6] J. Bondorf *et al.*, *Nucl. Phys. A* **333**, 285 (1980).
- [7] H. Tricoire, *Z. Phys. A* **312**, 221 (1983).
- [8] A. Diaz-Torres *et al.*, *Phys. Rev. Lett.* **98**, 152701 (2007).
- [9] V. Zagrebaev, *Ann. Phys.* **197**, 33 (1990).
- [10] L.R. Gasques *et al.*, *Phys. Rev. C* **74**, 064615 (2006) and references therein.
- [11] G.D. Dracoulis *et al.*, *J. Phys. G: Nucl. Part. Phys.* **23**, 1191 (1997).
- [12] F.S. Zhang *et al.*, *Front. Phys.* **13**, 132113 (2018) and references therein.
- [13] P.P. Singh *et al.*, *Phys. Lett. B* **671**, 20 (2009) and references therein.
- [14] A. Sood *et al.*, *Phys. Rev. C*, under revision.
- [15] A. Gavron, *Phys. Rev. C* **21**, 230 (1980).